

Stacking reversal as a source of perpendicular magnetic anisotropy in Ni-Pt multilayers

O. Robach,¹ C. Quirós,¹ H. Isérn,¹ P. Steadman,² K. F. Peters,³ and S. Ferrer¹¹European Synchrotron Radiation Facility, BP 220, F-38043 Grenoble, France²Department of Physics and Astronomy, University of Leeds, Leeds, LS2 9JC, United Kingdom³Hewlett Packard, 1000 NE Circle Blvd, Corvallis, Oregon 97330-4239, USA

(Received 23 April 2003; published 23 June 2003)

Based on surface x-ray diffraction and resonant magnetic surface x-ray diffraction measurements on ultra-thin films of Pt on Ni(111) and Ni on Pt(111), we propose a simple explanation for the perpendicular magnetic anisotropy (PMA) observed at room temperature in Ni-Pt multilayers. The stacking sequence of Ni grown on Pt(111) is the same as that of the Pt substrate (normal stacking: $ABCABC$) whereas that of Pt grown on Ni(111) is reversed ($ACBACB$). As a consequence the Ni layers in Ni-Pt multilayers alternate between normal and reversed stacking. The $[111]$ direction, which is normal to the interface planes, is invariant under the two types of stacking whereas the other equivalent crystallographic directions are not. This specific symmetry selects the $[111]$ direction as the preferred magnetic easy axis over all the multilayer stack, causing PMA. The influence of the Pt layer thickness on the PMA is also discussed.

DOI: 10.1103/PhysRevB.67.220405

PACS number(s): 75.70.-i, 68.55.-a

The Pt-Ni system has recently attracted attention since Pt-Ni multilayers exhibit perpendicular magnetic anisotropy (PMA) at room temperature (RT).^{1,2} In contrast to Co-Pt multilayers, where PMA appears when the magnetic Co layers are very thin, for Pt-Ni multilayers, PMA at RT only exists when the Pt layers are very thin (~ 2 atomic layers). For Co-Pt, PMA is generally agreed to be the result of the dominating contribution of the spin-orbit energy of interface Pt atoms over the dipolar energy, which favors parallel anisotropy, and becomes more important at increasing Co film thickness. The case of Pt-Ni is less clear. On the atomic level, Wilhelm *et al.*³ showed, using x-ray magnetic circular dichroism (XMCD), that the PMA in Ni_2Pt_2 multilayers at 10 K is associated with an anisotropy $\Delta\mu_L$ of the Ni orbital moment. They proposed, as Bruno already did on a theoretical basis,⁴ that the PMA is caused by this $\Delta\mu_L$. On the mesoscopic level, Shin *et al.*² attributed the PMA in Pt-Ni multilayers to a “bulklike” magnetoelastic effect in the Ni layers, that are under tensile stress. However, their model did not explain why very thin Pt layers are necessary for PMA. Angelakaris *et al.*¹ suggested that this was related to the requirement of Pt pseudomorphism with the Ni lattice: as soon as the Pt thickness exceeds one atomic layer, pseudomorphism is lost and Pt relaxes towards its bulk lattice parameter. However, the link between pseudomorphic Pt and PMA was not established.

In this Communication, we propose that, in Pt-Ni multilayers with very thin Pt layers, there is another structural contribution to the PMA, which is the stacking reversal. We also propose an explanation for the need of very thin Pt layers. We will describe the effect first and show its experimental basis later.

The idea is the following. Upon growing Pt-Ni multilayers, Pt and Ni, which have a fcc structure, both grow with the $[111]$ axis along the growth direction, since the (111) faces are the most stable. The two materials can a priori grow either with an $ABCABC\dots$ stacking of the (111) planes, or a $ACBACB\dots$ stacking. Usually, in most metallic systems, films tend to grow with the same stacking sequence as the substrates. This is not the case for the Pt-Ni system since,

whereas Ni on Pt(111) grows with the stacking sequence of the Pt substrate (normal growth), Pt on Ni(111) grows with reversed stacking, as will be shown later on. As a consequence, Ni-Pt multilayers, which contain both Ni on Pt and Pt on Ni layers, will exhibit alternate packing sequences of the Ni layers as normal/reverse/normal/reverse.

We assume that the axes of easy magnetization in the Ni layers are the same as in bulk Ni, i.e., the $[111]$ -type directions. Among the four $[111]$ -type directions, one of them, the $[111]$, is perpendicular to the surface of the films. The other three make angles of 19° with the surface plane. If the stacking sequence changes from normal to reverse, all $[111]$ -type directions undergo a reflection with respect to the (111) plane, which leaves the $[111]$ direction unchanged but rotates the three other directions. Fig. 1(a) shows as an example, the

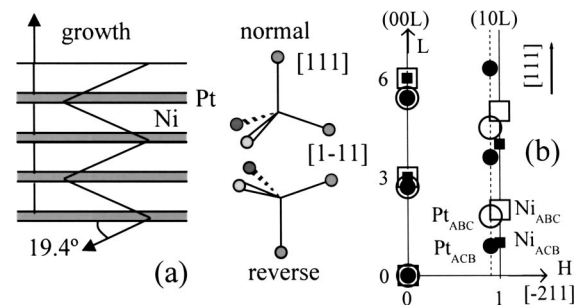


FIG. 1. (a) Schematic structural model of a Pt-Ni multilayer, used to explain the origin of PMA. The stacking reversal ($ABCABC\dots \Rightarrow ACBACB\dots$) of the (111) planes, observed for Pt on Ni, but not for Ni on Pt, leads to successive Ni layers having reversed stacking sequences. Among the four $\langle 111 \rangle$ easy magnetization axes of the Ni, only the one perpendicular to the surface is continuous through the whole multilayer. The other three, which are close (within 19°) to parallel to the surface, rotate at each new Ni layer. (b): side view of the reciprocal lattice for Pt on Ni(111), in the $(H 0 L)$ plane. L and H are respectively the Miller indexes in directions perpendicular and parallel to the surface (Ni lattice units). Empty (solid) squares: Ni Bragg peaks with ABC (ACB) stacking; empty (solid) circles: Pt Bragg peaks with ABC (ACB) stacking. The different locations in the Pt rod of the two stacking sequences allows to identify the one that is actually occurring.

zig-zag that the $[1-11]$ axis (which is in the plane of the figure) makes when going from one stacking sequence to the next. Suppose now that the magnetization within a Ni layer with normal stack is parallel to the $[1-11]$ direction, that we design as $[1-11]_{\text{normal}}$. Then, in the next Ni layer, the magnetization will not be able to remain in the same direction, because the $[1-11]_{\text{normal}}$ is no more an axis of easy magnetization in this layer. To be aligned with the easy axis the magnetization will have to rotate by at least 38° between the “normal” and “reversed” Ni layers, which implies the appearance of a domain wall at the interface between the two Ni layers. This is energetically unfavorable compared to a uniform magnetization, due to the excess exchange energy stored in the wall. In contrast, if the magnetization in a ‘normal’ Ni layer is along the $[111]$ axis, which is perpendicular to the surface, it will be able to remain in the same direction in a “reversed” Ni layer since the $[111]$ axis is continuous over the whole multilayer. The configuration with perpendicular magnetization is therefore stabilized with respect to the configurations with non-zero components of the parallel magnetization, leading to PMA. Why does the thickness of the Pt films have to be less than two atomic layers in order to have PMA? As will be shown later, at the Pt-Ni interface, the magnetization of the Pt atoms is essentially concentrated in the Pt plane in contact with the Ni, the next Pt plane has a magnetization at least three times smaller. Therefore, Pt layers with a thickness of two atomic planes or less will be magnetic over their whole thickness, while thicker Pt layers will have a central part that is non-magnetic (or much less magnetic).

The idea is that Pt layers with a nonmagnetic central part favor parallel magnetization with respect to perpendicular magnetization, for two reasons. First, and this is true for any multilayer, the magnetic/nonmagnetic Pt interfaces are a source of magnetic dipoles in the case of perpendicular magnetization, and their magnetostatic energy destabilizes the perpendicular configuration. Second, nonmagnetic Pt layers reduce the tendency of stacking reversal to induce PMA, since the two adjacent Ni layers are no more exchange-coupled and the notion of a domain wall in between them does not apply any more.

To summarize, we propose that PMA originates from the periodic stacking reversal of the Ni layers, and from the direct magnetic coupling between the Ni layers that is provided by very thin Pt layers. In what follows, we will describe first the structural data, which evidence the stacking reversal for Pt on Ni and the stacking conservation for Ni on Pt and second, the magnetic data, which reveal that there is only one magnetic Pt plane at the Pt-Ni interface, both for Pt on Ni and for Ni on Pt. In our experiments we did not investigate multilayer stacks but only single interfaces.

The experiments were performed on the ID03 surface diffraction beamline of the ESRF.⁵ The samples consisted of ultrathin [1–8 monoatomic layers (MLs)] Pt films grown on a Ni(111) single crystal, and of a thin (8 ML) Ni film grown on a Pt(111) single crystal. They were all grown by electron beam deposition (deposition rate: 1 ML/30 min for Pt, 1 ML/8 min for Ni) and characterized *in situ*, in the ultra high vacuum chamber mounted on the diffractometer. The struc-

ture of the films was studied using standard surface x-ray diffraction (SXRD).⁶ The details of the structural study will be presented elsewhere.⁷ The magnetic properties of the interface were investigated by resonant magnetic surface x-ray diffraction (RM-SXRD) (Ref. 8) near the Pt L_{III} edge (11.564 KeV). This technique allows to determine the profile of magnetic moment in the Pt across the interface, and also to measure the element-specific Pt magnetization curves. It is based on the fact that, when the energy of the x rays is precisely tuned to excite dipolar transitions in the Pt atoms (in our case $2p-5d$) the atomic scattering factor becomes slightly dependent on the Pt magnetic moment^{8,9} through a term that we design as n_m . As shown by de Bergevin *et al.*⁹ in a Co-Pt single crystalline alloy and also verified by us on Ni₉₀Pt₁₀,⁷ n_m is approximately proportional to the magnetic moment of the Pt atoms, with $n_m/\mu_{Pt}(\mu_B) = 2.4$. At the resonance energy, the diffracted intensity at a point (HKL) of reciprocal space contains a small magnetic contribution that may be extracted by measuring the asymmetry ratio, $R(HKL) = (I_\uparrow - I_\downarrow)/(I_\uparrow + I_\downarrow)$. I_\uparrow (respectively I_\downarrow) is the intensity measured at (HKL) upon applying an external magnetic field pointing up (resp. down). The experimental geometry is shown in the inset of Fig. 3. More details about the method can be found in Refs. 8 and 9.

We will first present the structural results. Pt is known to grow on Ni(111) in a parallel epitaxy.¹⁰ Diffraction measurements (not shown) of the in-plane reciprocal lattice revealed that most of the Pt grows non-pseudomorphic on the Ni substrate: it is almost completely relaxed from the beginning of the growth. Also, the widths of the in-plane peaks indicated that the diffracting domains had dimensions of more than 100 Å. Figure 1(b) shows a schematic side view of the reciprocal space of Pt and Ni considering the +11.3% lattice mismatch between both elements. The figure shows the expected locations of the Bragg peaks of the Pt film. The stacking sequence (ABC... or ACB...) of the Pt planes on the Ni can be determined by measuring the diffracted intensity along the Pt rod [located at $(0.9\ 0\ L)$], and comparing it to the neighboring $(10L)$ Ni crystal truncation rod⁶ (CTR) as shown in Fig. 2(a). As may be seen, both stackings of the Pt are present, with a net predominance (a factor ~ 10) of the reversed stacking. The Pt peaks at $(0.9\ 0\ 0.9)$ (inversed stacking) and $(0.9\ 0\ 1.8)$ (normal stacking) had the same width along L indicating that the thickness of each type of stacking was the same. Thus, it appears that, if an area of the film adopts at the early stages of growth a given stacking sequence, it maintains it during all the growth. Figure 2(b) is the equivalent of Fig. 2(a) but for the reverse growth of Ni on Pt(111) (which grows with its own in-plane lattice spacing). It shows that, in an eight-layer Ni film on Pt(111), again both stackings are present, but this time with a dominance of the normal stacking by a factor of ~ 3 . The films corresponding to Figs. 2(a) and 2(b) are both grown at RT. This tendency toward stacking reversal for Pt on Ni and stacking conservation for Ni on Pt has in fact already been observed by Staiger *et al.*¹¹ in molecular beam epitaxy grown Pt-Ni multilayers. The high-resolution-transmission-electron micrographs¹¹ in side view also showed that Ni and Pt layers

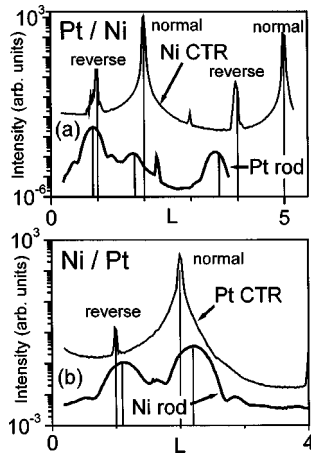


FIG. 2. SXR D data showing the stacking reversal for Pt on Ni(111) (a) and the stacking conservation for Ni on Pt(111) (b). (a) The Ni(10L) CTR (thin line) measured on the clean Ni substrate is compared to the neighboring (0.916 0 L) rod (thick line) of the Pt film, measured on a eight-layer film. (b) The (10L) CTR (thin line) of the Pt substrate is compared to the neighboring (1.1 0 L) rod (thick line) of the Ni film, both measured on a eight-layer Ni film.

consisted of columns with a single stacking sequence over the layer thickness, consistently with our results.

The magnetism of the Pt was probed, as mentioned above, with RM-SXR D. From the dependence of the diffracted intensity on the magnitude of the applied magnetic field,¹² it was found that both the Pt films on Ni and the Ni film on Pt have an in-plane (i.e., parallel) easy magnetization axis. This means that the sample is magnetically saturated in-plane when measuring the R factors. This is important to obtain the “full” value of the Pt magnetic moment, since we measure only its in-plane component in our geometry.

To determine how the magnetic moment of the Pt atoms varies along the direction z normal to the interface, we measured “magnetic rods.” These are profiles of $R(L)$ at fixed H and K , along the diffraction rods of the film or of the substrate. The influence of the different structural and magnetic parameters on the magnetic rods can be seen from the following equation:

$$R(L) \approx 2 \frac{|\tan(2\theta(L))|}{|F_{00L}(L)|} \sum_n \{ \text{occ}(n) \cdot n_m(n) \cos[-\varphi_{00L}(L) + 2\pi Lz(n)] \},$$

which describes the $R(L)$ profile for the (00L) rod, for a Pt film on Ni. The sum is taken over the n Pt planes of the film [occupation $\text{occ}(n)$, “magnetic moment” $n_m(n)$, z position $z(n)$]. θ is the Bragg angle. $|F_{00L}|$ and φ_{00L} are, respectively, the modulus and phase of the “nonmagnetic” structure factor, which includes contributions from both the Ni substrate and the Pt film. The data analysis is done in two steps: first we measure and analyze the standard crystallographic rod [$I(L) = |F_{HKL}(L)|^2$], to find an atomic model of the interface (atomic positions and site occupations). The structural model is then used as input to fit the measured $R(L)$ and to deduce n_m for the different Pt layers. This fit of $R(L)$ is relatively simple since the contributions $R_n(L)$ of the differ-

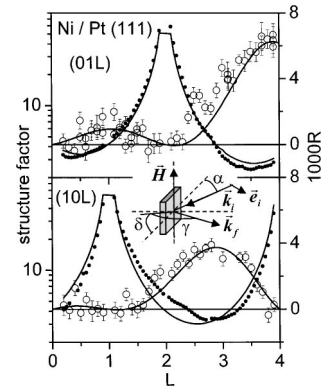


FIG. 3. Nonmagnetic (solid circles) and magnetic (open circles) Pt CTRs, for the Ni film on Pt(111). Lines: calculated rods. Inset: geometry for magnetic diffraction: the incident beam k_i and the incident linear polarization e_i are horizontal. The sample surface and the applied magnetic field H are vertical. α , γ and δ are the diffractometer angles.

ent magnetic Pt planes to the total R factor are additive, and each is proportional to $n_m(n)$.

Figure 3 shows the nonmagnetic and magnetic (01L) and (10L) truncation rods of the Pt substrate, for the eight-layer Ni film grown on Pt(111) at RT. The lines for the nonmagnetic rods are a fit with a bulk-terminated Pt(111) surface,¹³ with a 1.5 Å rms roughness. The lines for the magnetic rods are a fit in which only the topmost Pt plane is magnetic and has a n_m of 0.14. The other atoms of the Pt substrate are nonmagnetic ($n_m=0$). Putting a nonzero n_m in the Pt plane before last would add oscillations of shorter period in the magnetic rods, which are not present in the data. From this analysis, the Pt magnetic moment is 0.06 $\mu\text{B}/\text{atom}$ in the topmost Pt plane, and zero (or similar to the error bar $\sim 0.01 \mu\text{B}$) in the Pt planes below. Figure 4 shows the nonmagnetic (a) and magnetic (b) (00L) (i.e., specular) rods measured at RT for a four-layer Pt film grown at 150 K on Ni(111). The few R values measured both at 150 K and RT did not show any change with temperature. This indicates

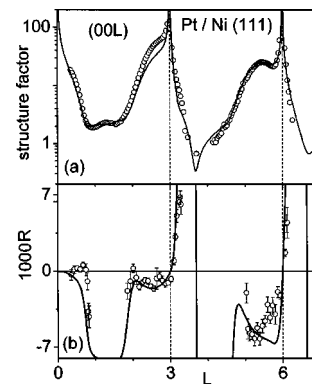


FIG. 4. Nonmagnetic (a) and magnetic (b) (00L) rods, measured on a four-layer Pt film grown at 150 K on Ni(111). Lines: calculated rods. The atomic model is a bulk-terminated flat Ni(111) single crystal, surmounted by a Pt film with $d_{\text{Pt-Ni}} = 2.10$ Å, $d_{\text{Pt-Pt}} = 2.28$ Å (bulk 2.265 Å) and occupations of (0.65, 0.58, 0.39, 0.17, and 0.04) for the first five Pt planes. The magnetic model comprises only one magnetic Pt plane (the first one) with $n_m = 0.3$.

that the Curie temperature is far above RT, so that the magnetic moment deduced from Fig. 4 is a good approximation of the one at 0 K. The line in Fig. 4(a) is a fit with a bulk terminated Ni surface covered by an imperfectly flat Pt layer. The line on Fig. 4(b) is a fit with only the interfacial Pt plane of the film being magnetic, with $n_m = 0.3$. The Pt planes above have $n_m = 0$. A fit of similar quality can be obtained by taking the same total $n_m = 0.3$, but putting 75% of it in the first Pt plane ($n_{m1} = 0.225$) and 25% of it in the second Pt plane ($n_{m2} = 0.075$). The error bars on the magnetic moment profile are therefore larger than for Ni on Pt. This comes from the large number of parameters in the structural model, which induces some imprecision on the phase of the structure factor. From this analysis, the total Pt moment is $(0.12 \pm 0.01)\mu\text{B}$, with 100% to 75% of it in the first Pt plane, and 0% to 25% of it in the second Pt plane.

The analysis of Figs. 3 and 4 shows that in both cases ($\text{Ni}_8/\text{Pt}_{\text{BULK}}$ and $\text{Pt}_4/\text{Ni}_{\text{BULK}}$), the magnetic moment induced in the Pt is essentially confined to the Pt plane in contact with the Ni. The total moment in the Pt is about two times larger for Pt on Ni ($0.12\mu\text{B}$) than for Ni on Pt ($0.06\mu\text{B}$). It is not clear yet if this difference is due to the structural asymmetry between the two growths (regarding strain,⁷ and stacking), or simply to a possibly lower Curie temperature of the thin Ni film,¹⁴ compared to bulk Ni (the $\text{Ni}_8/\text{Pt}_{\text{BULK}}$ measurements were done only at RT). In order to apply our results on the $\mu_{\text{Pt}}(z)$ profile for $\text{Ni}_8/\text{Pt}_{\text{BULK}}$ and $\text{Pt}_4/\text{Ni}_{\text{BULK}}$ to Ni_nPt_m multilayers, one has to assume that the $\mu_{\text{Pt}}(z)$ profile is independent of the Pt thickness, m , and of the Ni thickness, n . Using this assumption, our data show that only the Ni_nPt_2 multilayers have fully magnetized Pt layers. The same assumption was used in Ref. 9 to build magnetic moment profiles from “total μ_{Pt} ” and “total μ_{Ni} ” XMCD measurements on Ni_nPt_m multilayers with different m 's and n 's. Wilhelm *et al.*¹⁵ also used the additional assumption that the $\mu_{\text{Pt}}(z)$ profile is the same for the Pt on Ni and Ni on Pt interfaces.

Our results for Pt on Ni agree reasonably well with the results of *ab initio* calculations,¹⁵ which give magnetic moments of $0.11\mu\text{B}$, $0.05\mu\text{B}$, and $0.02\mu\text{B}$ per atom for the first

three Pt planes in a Ni_6Pt_5 multilayer. On the contrary, the agreement with the experimental XMCD results of Wilhelm *et al.*¹⁵ on a Ni_6Pt_2 multilayer is poor since these authors reported $0.29\mu\text{B}/\text{atom}$ for the average magnetic moment of the Pt, which is about a factor of 2 higher than ours. Such a discrepancy between the Pt moments derived from XMCD and RM-SXRD was already noted for the Co-Pt system, and is not yet explained.

In conclusion, a new structural contribution to the PMA of Ni/Pt multilayers has been proposed. It is based on the observed alternation of stacking sequences in the Ni layers caused by the Pt spacer, which privileges the direction of magnetization normal to the film. It has also been shown that the magnetism of the Pt atoms is essentially reduced to these in contact with the Ni planes, which favors the interlayer Ni coupling when the thickness of the Pt spacers is very small. From the point of view of the stacking, the Pt-Ni multilayer is analogous to a “polytypic” hexagonal Pt-Ni alloy, with the c axis perpendicular to the surface. The lower symmetry of this hexagonal lattice compared to the cubic fcc lattice should favor a large uniaxial anisotropy, as, for example, in hcp Co compared to fcc Co.¹⁶ If the stacking reversal induced PMA is strong enough, it should be possible to achieve thick perpendicular films by growing epitaxial Ni(111) and periodically reversing the stacking sequence of the Ni(111) planes. This could be achieved for example by introducing carbon atoms via an exposure to carbon monoxide: Ni_3C consists in a hcp stacking of Ni planes, intercalated with carbon planes, and a monoatomic carbon layer should favor the Ni stacking reversal. The perpendicular magnetic anisotropy observed in thick carbon-contaminated Ni films¹⁷ could possibly be related to this. Finally, it should be noted our model does not contradict the microscopic explanation of the PMA given by Wilhelm *et al.*³ Both structural effects, the stress,² and the stacking faults, may produce an anisotropy of the Ni orbital moment, as they reduce the symmetry of the Ni.

We thank E. Paisier, L. Petit, and A. Solé for technical assistance, and Y. Jugnet for lending us the Pt-Ni single crystal.

¹M. Angelakaris *et al.*, J. Appl. Phys. **82**, 5640 (1997).

²S. C. Shin *et al.*, Appl. Phys. Lett. **73**, 393 (1998); Y. S. Kim, and S. C. Shin, J. Magn. Magn. Mater. **198–199**, 602 (1999); Phys. Rev. B **59**, R6597 (1999); IEEE Trans. Magn. **34**, 858 (1998); G. Srinivas and S. C. Shin, J. Magn. Magn. Mater. **198–199**, 341 (1999); S. K. Kim *et al.*, Phys. Rev. B **64**, 052406 (2001).

³F. Wilhelm *et al.*, Phys. Rev. B **61**, 8647 (2000).

⁴P. Bruno, Phys. Rev. B **39**, 865 (1989).

⁵S. Ferrer and F. Comin, Rev. Sci. Instrum. **66**, 1674 (1995).

⁶I. K. Robinson, Phys. Rev. B **33**, 3830 (1986); S. R. Andrews and R. A. Cowley, J. Phys. C **18**, 6247 (1985); G. Renaud, J. Phys. III **4**, 69 (1994); E. Vlieg *et al.*, Surf. Sci. **210**, 301 (1989).

⁷O. Robach *et al.* (unpublished).

⁸S. Ferrer *et al.*, Phys. Rev. Lett. **77**, 747 (1996); S. Ferrer *et al.*, Phys. Rev. B **56**, 9848 (1997); J. Alvarez *et al.*, *ibid.* **60**, 10 193 (1999).

⁹F. de Bergevin *et al.*, Phys. Rev. B **46**, 10 772 (1992).

¹⁰J. A. Barnard and J. J. Ehrhardt, J. Vac. Sci. Technol. A **8**, 4061 (1990).

¹¹W. Staiger *et al.*, J. Mater. Res. **12**, 161 (1997).

¹²O. Robach *et al.*, Phys. Rev. B **65**, 054423 (2002).

¹³As there is little pseudomorphic Ni in the Ni films on Pt, as a first approximation the Ni film does not contribute to the diffracted intensity on the Pt (10L) and (01L) CTR's.

¹⁴C. A. Neugebauer and Z. Angew. Phys. **14**, 182 (1962); M. S. Cohen, in *Handbook on Thin Film Technology*, edited by L. I. Maissel and R. Glang (McGraw-Hill, New York, 1970), pp. 17–25.

¹⁵F. Wilhelm *et al.*, Phys. Rev. Lett. **85**, 413 (2000); F. Wilhelm, Ph.D thesis, de Berlin, 2000.

¹⁶F. Ono, J. Phys. Soc. Jpn. **50**, 2564 (1981); D. S. Rodbell, J. Appl. Phys. **33**, 1126 (1962); L. Néel, J. Phys. Radium **15**, 225 (1954); M. Farle, Rep. Prog. Phys. **61**, 755 (1998).

¹⁷G. N. Kakazei and N. A. Lesnik, J. Magn. Magn. Mater. **155**, 57 (1996).